

## **Altered Right Ventricular Filling on 4D Flow MRI in Young Adults Born Premature**

**THIS PAPER IS CURRENTLY UNDER REVIEW AT RADIOLOGY: CARDIOTHORACIC IMAGING**

P. A. Corrado, G. P. Barton, J. A. Macdonald, C. J. François, M. W. Eldridge, K. N. Goss, O. Wieben

**Summary statement:** We used 4D flow MRI to measure biventricular kinetic energy in adults born premature to investigate mechanisms of elevated heart failure risk. Preterm-born subjects had decreased right ventricular E/A kinetic energy ratio, suggesting altered diastolic filling relative to controls.

### **Key points:**

- We identified altered right ventricular diastolic function, including reduced E/A kinetic energy ratio, E/A peak filling rate ratio, and (nonsignificantly) E/A tricuspid valve flow ratio, in subjects born premature.
- The right ventricular E/A kinetic energy ratio was weakly correlated with stroke volume index and heart rate independently.
- Further study is needed to determine whether RV diastolic flow assessed by 4D flow MRI may serve as a predictive indicator of cardiovascular disease risk in young adults born premature.

### **List of abbreviations**

4D – four-dimensional; KE – kinetic energy; LV – left ventricle; RV – right ventricle; EDV – end diastolic volume; EDVi – end diastolic volume index; ESV – end systolic volume; ESVi – end systolic volume index; SV – stroke volume; SVi – stroke volume index; ESAi – end systolic area index; EDAi – end diastolic area index; EF – ejection fraction; CI – cardiac index; PFR – peak filling rate. E-wave – early diastolic filling; A-wave – late diastolic filling (atrial contraction). BSA – body surface area; BMI – body mass index; BP – blood pressure ;  $E'_L$ , viscous energy dissipation rate;  $E_L$ , net viscous energy dissipation.

## **Abstract**

### **Purpose**

Individuals born premature have smaller ventricles and an increased risk of heart failure by young adulthood, though whether this is linked to systolic or diastolic function remains unresolved. Here, we applied 4D flow MRI to measure intraventricular flow in young adults born premature to investigate mechanisms that may account for increased HF risk in this population.

### **Materials and Methods**

Fifty-six young adults participated in this prospective observational cardiac MRI study from 2016-2020: 35 subjects born moderately to extremely premature (birth weight <1500 g or gestational age ≤32 weeks; 12M/23F; age=25.9 ± 3.7 years), and 21 term-born subjects (10M/11F; age=25.1 ± 2.6 years). Subjects underwent cardiac MRI, including cine cardiac structure/function assessment and 4D flow MRI. In each ventricle, normalized kinetic energy (KE/EDV) and flow through the atrioventricular (AV) valve were computed and compared between term and preterm subjects at systolic and diastolic (E-wave and A-wave) time points using Wilcoxon rank sum tests.

### **Results**

Preterm-born subjects had decreased right ventricular (RV) E/A KE ratios (2.4 vs. 3.5, P<0.01) and decreased E/A peak filling rate ratios (computed from RV volume-time curves; 2.3 vs. 3.5, P=0.03). Additionally, viscous energy dissipation was increased during systole (5.7 vs. 4.2, P=0.03), A-wave (3.9 vs. 2.2, P=0.03), and summed over the cardiac cycle (2.4 vs. 1.9, P=0.02), in preterm relative to term subjects.

### **Conclusion**

Our results suggest that RV diastolic filling is altered in young adults born moderately to severely premature. These findings may relate to the previously reported early heart failure risk in this population.

## Introduction

Preterm births are steadily increasing in the United States and account for nearly half a million deliveries annually (1). Recent advances in the treatment of extremely premature infants have led to decreases in mortality (2), such that the long-term ramifications of premature birth are only now becoming apparent. A recent Swedish registry study of individuals born in the past 2 decades identified a 17-fold increased risk of developing heart failure by young adulthood in individuals born extremely premature (gestational age <28 weeks) (3). Premature birth is also associated with changes in cardiac morphology, including smaller ventricular chamber sizes and reduced stroke volume index (SVi) (4,5), and in some studies slightly reduced right ventricular (RV) ejection fraction (EF) (6). Additional studies demonstrate impaired cardiac reserve during exercise in adults born premature, including an attenuated stroke volume response during submaximal exercise (7,8) and a slower heart rate recovery after exercise (9). Despite these findings, hemodynamic insights into the mechanisms of exercise intolerance and increased risk for heart failure in individuals born premature is lacking.

4D flow cardiac MRI enables detailed investigation of intracardiac hemodynamics by measuring the 3D time-resolved blood velocity vector field in the heart throughout the cardiac cycle, making it a promising tool for probing subtle differences in cardiac function (10). In addition to flows through any number of retrospectively placed measurement planes, 4D flow MRI can be used to measure intraventricular kinetic energy (KE) (11) and viscous energy dissipation ( $E_L$ ) (12,13), which have been demonstrated as sensitive measures of cardiac function (14–19). Another benefit of the measuring intraventricular energetics is they can be used to assess both systolic and diastolic hemodynamics with a single scan: Studies have revealed reduced systolic

KE in myocardial infarction (20) and heart failure (18) patients, and 4D flow LV KE measures of diastolic function have shown good correlation with standard 2D phase-contrast mitral inflow metrics but with stronger independent correlations to age than 2D metrics (21).

In this study, we used 4D flow MRI to measure atrioventricular valve flow and biventricular KE and E<sub>L</sub> in young adults born premature during both systole and diastole in order to investigate the mechanisms of impaired cardiac function and reserve that may contribute to the increased risk of heart failure in this population. Our hypothesis was that young adults born premature have altered ventricular KE, E<sub>L</sub>, and atrioventricular valve flow compared to term-born controls.

## Materials and Methods

### Participants

A total of 70 young adults participated in cardiac MRI studies at our academic medical center from 2016-2020 (5), with baseline cardiac morphologic and functional data now published. In three subjects, the 4D flow scan was forgone due to scanner time limitations. In 11 subjects, the 4D flow data was unusable for various reasons (data lost during transfer, N=2; improper coil selection during scan prescription, N=3; severe arrhythmia or poor gating signal, N=2; artifacts present from motion or BMI>40 kg/m<sup>2</sup>, N=4), so 56 subjects were included in the analysis. Subjects born moderately to extremely premature (N=35) were recruited from either the Newborn Lung Project, a cohort of infants born premature between 1988 and 1991 in Wisconsin and Iowa (22) and followed prospectively from birth, or from the local population after verification of preterm birth history from neonatal records. Preterm subjects met either of the two inclusion criteria: 1) gestational age ≤32 weeks, or 2) birth weight <1500 g. Age-matched term-born participants (N=21) were recruited from the local population. All participants were

free of current cardiovascular or respiratory illness, nonsmokers, and without significant disabilities. All participants provided written informed consent in accordance with the protocol approved by the Institutional Review Board at our institution. Data were coded with subject and study-specific identification codes to ensure anonymity in a HIPAA-compliant manner and blinded analysis. Our sample size target was set at 60 according to power calculations based on systolic KE/EDV in heart failure patients from the study by Kanski et al (18), using a significance level of 0.05 and a power of 75%.

### **Cardiovascular Magnetic Resonance Imaging Acquisition**

Each subject underwent cardiac MRI on a clinical 3T MRI scanner (Discovery MR750, GE Healthcare, Waukesha, WI) or 3T PET-MRI scanner (GE Signa PET/MR Discovery 750W, GE Healthcare, Waukesha, WI) with an 8-channel phased-array cardiac coil. To characterize cardiac function, we acquired 2-dimensional, cine balanced steady-state free precession (bSSFP) images over several breath holds in short-axis and long axis (2-, 3-, and 4-chamber) views with field of view=35x35 cm; spatial resolution=1.4x1.4 mm; slice thickness=7 mm; acquired/reconstructed cardiac phases=20.

4D flow cardiac MRI was performed with a radially undersampled 4D flow sequence (phase contrast vastly-undersampled isotropic projection [PC VIPR (23)]: repetition time [TR]: 5.8-6.3 ms; echo time [TE]: 2.1-2.3 ms; velocity encoding [VENC] = 150-200 cm/s; imaging volume = 32x32x32 cm; spatial resolution = 2.5 mm isotropic, scan time = 9.3-9.6 minutes). Images were reconstructed offline with retrospective respiratory gating from an abdominal belt (50% efficiency), using compressed sensing (24) with a spatial-wavelet-transform L1-norm penalty ( $\lambda$  =

0.01). Retrospective ECG gating with spatial frequency dependent temporal interpolation was used for cine reconstruction, using twenty cardiac phases (25).

### **Cardiac MR Analysis**

The LV and RV cavities were manually segmented at each time frame on short-axis bSSFP images using Segment (Medviso, <http://segment.heiberg.se>; v2.0 R5399) (26). The contours were used to compute the following metrics, which were normalized by body surface area (BSA) (27) to control for the influence of subject size: end diastolic volume index (EDVi), end systolic volume index (ESVi), stroke volume index (SVi), and cardiac index (CI). E-wave and A-wave peak filling rates (PFR) were calculated from the volume-time curves as the maximum slopes of the diastolic volume-time curve before and after diastasis, respectively, and normalized by end diastolic volume (EDV) (28). Additionally, the contours of the left (on 2- and 4-chamber views) and right atrium (on 4-chamber view) was drawn manually at ES and ED time frames to compute ES and ED volumes (for LA via bi-plane method (29)) and areas (for RA). The short axis dataset, including the RV/LV segmentations, was then rigidly registered (using the ANTs software package (30)) to the 4D flow time-averaged magnitude image, and ventricular velocities were extracted for intraventricular flow analysis using the method proposed by Gupta et al (31). KE was then computed at each time frame by summing the KE contributions for all voxels in each ventricle:

$$KE_t = \sum_{ventricle} \frac{1}{2} \rho_{blood} V_{vox} v_{vox}^2$$

where  $\rho_{blood}$  is the density of blood (1.06 g/cm<sup>3</sup>),  $V_{vox}$  is the voxel volume,  $v_{vox}$  is the velocity magnitude, and the summation is over all voxels in the ventricle (11). Five 4D flow parameters, normalized by EDV to control for the impact of heart size, were extracted from the KE-time curve per ventricle: average KE/EDV, peak systolic KE/EDV, E-wave KE/EDV, A-wave KE/EDV, and the

ratio of E-wave KE to A-wave KE. The intraventricular viscous energy dissipation rate,  $E'_L$ , was similarly assessed at the same time points as well as the net energy dissipation over the whole cardiac cycle ( $E_L$ ) (12,32). Ventricular vorticity was also assessed at the same time points (33). Flow through the AV-valves were also computed at the E- and A-peaks (as well as the net flow over 1 cardiac cycle) using retrospective valve tracking to account for valve motion (34), providing alternative measurements of LV and RV PFR derived from the 4D flow data rather than the bSSFP volume-time curves.

### **Statistical Analysis**

Baseline anthropometric and MRI data were compared across birth status (preterm vs. term) using unpaired Wilcoxon Rank Sum Tests. Univariate linear regression was used to test correlation between the E/A KE ratio and SVi, heart rate, and EDVi. Significance level was determined a priori at the 0.05 level and all tests were 2-tailed. No correction for multiple comparisons was performed. All data is presented as mean (standard deviation), unless otherwise noted. All statistical analyses were performed in Excel (Microsoft Inc.; Redmond, Washington, USA; Version 16.35). The scripts and data from this study are available from the corresponding author upon reasonable request.

### **Results**

The average gestational age of subjects born premature was  $28.9 \pm 2.7$  weeks, with an average birth weight of  $1160 \pm 250$  g. Baseline anthropomorphic measures and blood pressures are shown in Table 1. On average, preterm-born subjects were shorter, but body weight, body mass index (BMI), and body surface area (BSA) were not significantly different.

## **Cardiac MRI Structure and Function**

Standard measures of cardiac morphometry and function including strain in this population have been previously published (5), and metrics reported here are for the subset of individuals for whom 4D flow sequences were available (Table 2). Compared to term-born subjects, preterm-born subjects had lower indexed stroke volumes, as previously reported (5). Both ventricles had normal ejection fraction in the preterm group. LV diastolic function, as measured by E- and A-wave PFR/EDV (derived from volume-time curves), was not significantly different in preterm vs. term subjects. RV diastolic function, however, was altered in preterm subjects, with increased A-wave PFR/EDV and decreased ratio of E-wave to A-wave PFR (derived from volume-time curves). To further characterize cardiac structure and function, we also measured atria sizes. LA ESVi and SVi were significantly reduced in the preterm group ( $P<0.01$  and  $P=0.01$ , respectively), while none of the RA area metrics differed significantly between groups.

## **4D Flow MRI KE, E<sub>L</sub>, and AV Valve Flow**

4D Flow CMR measures are shown in Table 3, and average KE-time curves for each group are shown in Figure 1. Average and peak systolic KE/EDV were not significantly different between term and preterm subjects. There were, however, significant differences in diastolic KE (Figure 2). Compared to term-born subjects, preterm-born subjects had higher A-wave KE/EDV ( $P=0.05$ ) and lower E/A KE ratios in the RV ( $P<0.01$ ). Similar but not significant trends were seen in the LV. The highly correlated (Supplemental Figure 1) vorticity measures show similar results and are included as Supplemental Table 1. There were no significant differences in flow through either valve between groups, but the ratio of E- to A-wave flow through the tricuspid valve derived from 4D flow data trended lower in preterm subjects ( $P=0.07$ ). Net viscous energy dissipation was

higher in the RV's of preterm subjects than term subjects ( $P=0.02$ ), with elevated  $E'_L$  during both systole and diastole.

### **Kinetic Energy Correlations**

As the E/A KE ratio was found to be the 4D flow metric most affected by preterm birth status, we evaluated for correlations of the E/A KE ratio with SVi and heart rate. In univariate regression, E/A KE ratio was positively correlated with SVi and negatively correlated with heart rate in both ventricles (Figure 3). In multivariate regression, RV E/A KE ratio was independently associated with both SVi (slope=0.060  $m^2/mL$ ; slope CI=[0.015, 0.106]  $m^2/mL$ ;  $P=0.01$ ) and HR (slope=0.039  $bpm^{-1}$ ; slope CI=[0.005, 0.073]  $bpm^{-1}$ ;  $P=0.03$ ).

### **Discussion**

Prior studies demonstrate significantly smaller chamber size with preserved global cardiac function in adolescents and adults born premature using standard cardiac MRI measures (4–6). Additional studies also report mild pulmonary hypertension (8), impaired cardiac reserve to exercise (8,9), and subtle right ventricular-pulmonary vascular uncoupling in adults born premature (35). Here, we applied 4D flow MRI to measure intraventricular kinetic energy, viscous energy dissipation, and flow in young adults born premature to further investigate the mechanisms of impaired cardiac function and reserve. We identified altered RV flow, particularly during diastole, including reduced E/A KE ratio, E/A PFRand viscous energy dissipation in subjects born premature.

Our findings regarding diastolic function in the preterm population are consistent with other reports in adults born premature, though we are the first to assess this with 4D flow specifically. Five echocardiography-based studies in children (age 6-18) report no significant differences in LV

diastolic function (36–40). On the other hand, one study in adults born premature using echocardiography demonstrated impaired diastolic strain rate in the LV (4). In our results, no significant differences in LV diastolic flow were observed, but there was a trend towards reduced LV E/A KE ratio ( $P=0.06$ ). In the RV, on the other hand, we did observe differences in diastolic flow. The largest prior pediatric echo study to address RV function reported a trend toward reduced TV E/A velocity ratio ( $p=0.06$ ), in association with significantly higher estimated pulmonary artery pressures and tricuspid annular plane systolic excursion ( $p=0.001$ ) (41).

Reduced RV diastolic KE E/A ratio correlated with stroke volume and heart rate. We suspect that the elevated heart rate partially causes a reduction in the E/A KE ratio through reduced filling time, limiting the time available for passive filling and increasing the reliance on atrial contraction. We also suspect that the reduced SV is caused at least partially by the altered RV diastolic filling through decreased EDV and preload. However, as this is an observational study, we cannot definitively comment on causality between physiological factors. There are likely other physiological contributors to the observed KE differences as well. Circumferential strain analysis has previously revealed hypercontractile adult preterm hearts that reached peak systole and end diastole much later in the cardiac cycle, particularly in the RV (5). This delayed relaxation could have led to the increased reliance on A-wave rather than E-wave filling in preterm subjects revealed herein. The study by Lewandowski et al., on the other hand, reported a hypocontractile strain pattern in adults born preterm (4), highlighting the heterogeneity of preterm heart development and the need for clarifying studies. Two studies in animal models of premature birth found increased interstitial fibrosis relative to term-born controls (42,43). If confirmed in humans, fibrosis-associated stiffness could explain the observed differences in diastolic KE.

Another possible physiological mechanism affecting diastolic function could be myocardial fiber orientation (44), although more data are needed in this area in animals and humans. Further investigation into the mechanisms of altered RV diastolic function in the human preterm heart will be required to assess for increased myocardial stiffness and fibrosis as well as myocyte-level dysfunction such as impaired calcium handling.

We also uncovered differences between term and preterm groups in the related parameter, viscous energy dissipation, with elevated viscous energy dissipation in preterm subjects during systole, diastole, and summed over the full cardiac cycle. This parameter measures the amount of kinetic energy that is converted to thermal and acoustic energy through fluid viscosity and thus is not capable of being recovered as potential energy (pressure) downstream (12). A possible cause of this increased viscous energy loss is the decreased RV length (6) which may alter flow fields in a way that reduces energy conversion efficiency. We also hypothesize that the increased RV A-wave KE is partially a result of the need to compensate for viscous energy loss in the RV of preterm subjects by adding more energy to the system through RA contraction.

Finally, we measured atrial sizes, finding smaller LA volumes in preterm subjects and no significant differences in RA area. This is consistent with a smaller preterm heart overall, as several studies have noted smaller ventricular volumes (4–6). That RA sizes were not significantly different between groups may reflect reduced sensitivity in the RA measurement caused by only having one bSSFP imaging plane containing the RA. Alternatively, it could result from early RA enlargement to compensate for impaired RV filling, resulting in comparable RA sizes among groups despite smaller hearts overall in the preterm group. However, since not finding a

significant difference in RA area does not prove that the areas are the same, these are only speculative hypotheses at this point.

This study highlights the capability of 4D flow MRI to detect subtle differences in cardiac function by measuring hemodynamic parameters that are not captured with traditional cardiac function metrics. Here, three measures of diastolic flow in the RV, including the E/A KE ratio ( $P<0.01$ ), the cine bSSFP E/A PFR ratio ( $P=0.03$ ), and the 4D-flow derived TV E/A flow ratio ( $P=0.07$ ) tend to coalesce around mild RV diastolic dysfunction in the preterm heart. As altered cardiac function at baseline is thought to make some premature individuals less able to withstand acute perturbations such as myocarditis or myocardial infarction thereby leading to elevated early heart failure rates (45), 4D flow MRI may prove useful as a clinical marker for subjects born extremely premature with higher risk of early cardiovascular disease. However, longitudinal studies are needed to assess whether 4D flow-derived measures of diastolic flow can predict subsequent cardiovascular disease.

Our study has several limitations. First, we did not collect echocardiographic images in these patients, precluding comparison with more traditional measures of diastolic function. However, MRI is the gold standard imaging modality for cardiac structure and function, and 4D flow MRI is emerging as a powerful complementary tool for uncovering subtle dysfunction (19,46,47). A second limitation is that two different MRI scanners were used, which may have had a slight impact on 4D flow measurements through differential gradient performance. However, each scanner was used in a similar proportion in each group and the use of multiple scanners makes this study more generalizable, as one of any number of scanners could be used to assess ventricular KE in a clinical setting should this technique someday be used for diagnosis or risk

estimation. Additionally, a higher temporal resolution would have improved the accuracy of measurements based on volume-time curves and KE-time curves, but we were limited by finite scan time, so we acquired 20 cardiac frames for all sequences.

In summary, we used 4D flow MRI to measure intraventricular hemodynamics in the LV and RV of young adults born moderately to extremely premature, demonstrating altered diastolic RV KE in this group compared to term-born controls. Additional studies are needed to investigate the mechanisms of diastolic flow alterations and whether 4D flow KE measures of diastolic function are predictive of future cardiovascular disease in this high-risk population.

## References

1. Ferré C, Callaghan W, Olson C, Sharma A, Barfield W. Effects of Maternal Age and Age-Specific Preterm Birth Rates on Overall Preterm Birth Rates — United States, 2007 and 2014. *MMWR Morb Mortal Wkly Rep.* 2016;65(43):1181–1184.
2. Younge N, Smith PB, Gustafson KE, et al. Improved survival and neurodevelopmental outcomes among extremely premature infants born near the limit of viability. *Early Hum Dev.* Elsevier Ireland Ltd.; 2016;95:5–8.
3. Carr H, Cnattingius S, Granath F, Ludvigsson JF, Edstedt Bonamy AK. Preterm Birth and Risk of Heart Failure Up to Early Adulthood. *J Am Coll Cardiol.* 2017;69(21):2634–2642.
4. Lewandowski AJ, Augustine D, Lamata P, et al. Preterm Heart in Adult Life. *Circulation.* 2013;127(2):197–206.
5. Goss KN, Haraldsdottir K, Beshish AG, et al. Association Between Preterm Birth and Arrested Cardiac Growth in Adolescents and Young Adults. *JAMA Cardiol.* 2020;5(8):910.
6. Lewandowski AJ, Bradlow WM, Augustine D, et al. Right ventricular systolic dysfunction in young adults born preterm. *Circulation.* 2013;128(7):713–720.
7. Huckstep OJ, Williamson W, Telles F, et al. Physiological Stress Elicits Impaired Left Ventricular Function in Preterm-Born Adults. *J Am Coll Cardiol.* 2018;71(12):1347–1356.
8. Goss KN, Beshish AG, Barton GP, et al. Early pulmonary vascular disease in young adults born preterm. *Am J Respir Crit Care Med.* 2018;198(12):1549–1558.
9. Haraldsdottir K, Watson AM, Beshish AG, et al. Heart rate recovery after maximal exercise is impaired in healthy young adults born preterm. *Eur J Appl Physiol.* Springer Berlin Heidelberg; 2019;119(4):857–866.
10. Markl M, Frydrychowicz A, Kozerke S, Hope M, Wieben O. 4D Flow MRI. *J Magn Reson Imaging.* 2012;36(5):1015–1036.
11. Carlsson M, Heiberg E, Toger J, Arheden H. Quantification of left and right ventricular kinetic energy using four-dimensional intracardiac magnetic resonance imaging flow measurements. *AJP Hear Circ Physiol.* 2012;302(4):H893–H900.
12. Barker AJ, Van Ooij P, Bandi K, et al. Viscous energy loss in the presence of abnormal aortic flow. *Magn Reson Med.* 2014;72(3):620–628.
13. Kamphuis VP. Scan – rescan reproducibility of diastolic left ventricular kinetic energy , viscous energy loss and vorticity assessment using 4D flow MRI : analysis in healthy subjects. *Int J Cardiovasc Imaging.* Springer Netherlands; 2018;34(6):905–920.
14. Garg P, Van Der Geest RJ, Swoboda PP, et al. Left ventricular thrombus formation in myocardial infarction is associated with altered left ventricular blood flow energetics. *Eur Heart J Cardiovasc Imaging.* 2019;20(1):108–117.
15. Eriksson J, Bolger AF, Ebbers T, Carlhäll CJ. Four-dimensional blood flow-specific markers

- of LV dysfunction in dilated cardiomyopathy. *Eur Heart J Cardiovasc Imaging*. 2013;14(5):417–424.
16. Rutkowski DR, Barton G, François CJ, Bartlett HL, Anagnostopoulos P V., Roldán-Alzate A. Analysis of cavopulmonary and cardiac flow characteristics in fontan Patients: Comparison with healthy volunteers. *J Magn Reson Imaging*. 2019;49(6):1786–1799.
  17. Wong J, Chabiniok R, DeVecchi A, et al. Age-related changes in intraventricular kinetic energy: a physiological or pathological adaptation? *Am J Physiol - Hear Circ Physiol*. 2016;310:H747–H755.
  18. Kanski M, Arvidsson PM, Töger J, et al. Left ventricular fluid kinetic energy time curves in heart failure from cardiovascular magnetic resonance 4D flow data. *J Cardiovasc Magn Reson. Journal of Cardiovascular Magnetic Resonance*; 2015;17(1):1–10.
  19. Han QJ, Witschey WRT, Fang-Yen CM, et al. Altered right ventricular kinetic energy work density and viscous energy dissipation in patients with pulmonary arterial hypertension: A pilot study using 4D flow MRI. *PLoS One*. 2015;10(9):1–14.
  20. Garg P, Crandon S, Swoboda PP, et al. Left ventricular blood flow kinetic energy after myocardial infarction - insights from 4D flow cardiovascular magnetic resonance. *J Cardiovasc Magn Reson 2018* 201. *Journal of Cardiovascular Magnetic Resonance*; 2018;20(61):61.
  21. Crandon S, Westenberg JJM, Swoboda PP, et al. Impact of Age and Diastolic Function on Novel, 4D flow CMR Biomarkers of Left Ventricular Blood Flow Kinetic Energy. *Sci Rep*. 2018;8(1):1–11.
  22. Palta M, Gabbert D, Fryback D, et al. Development and validation of an index for scoring baseline respiratory disease in the very low birth weight neonate. *Pediatrics*. 1990;86(5):714–721.
  23. Gu T, Korosec FR, Block WF, et al. PC VIPR: A high-speed 3D phase-contrast method for flow quantification and high-resolution angiography. *Am J Neuroradiol*. 2005;26:743–749.
  24. Lustig M, Donoho D, Pauly JM. Sparse MRI: The application of compressed sensing for rapid MR imaging. *Magn Reson Med*. 2007;58(6):1182–1195.
  25. Liu J, Redmond MJ, Brodsky EK, et al. Generation and visualization of four-dimensional MR angiography data using an undersampled 3-D projection trajectory. *IEEE Trans Med Imaging*. 2006;25(2):148–157.
  26. Tufvesson J, Hedstrom E, Steding-Ehrenborg K, Carlsson M, Arheden H, Heiberg E. Validation and Development of a New Automatic Algorithm for Time-Resolved Segmentation of the Left Ventricle in Magnetic Resonance Imaging. *Biomed Res Int*. 2015;2015:1–12.
  27. Mosteller RD. Simplified calculation of body-surface area. *N Engl J Med*. 1987;317(17):1098.
  28. Westenberg JJM. CMR for Assessment of Diastolic Function. *Curr Cardiovasc Imaging Rep*.

2011;4(2):149–158.

29. Kowallick JT, Kutty S, Edelmann F, et al. Quantification of left atrial strain and strain rate using Cardiovascular Magnetic Resonance myocardial feature tracking: a feasibility study. *J Cardiovasc Magn Reson.* 2014;16(1):60.
30. Avants BB, Tustison NJ, Stauffer M, Song G, Wu B, Gee JC. The Insight ToolKit image registration framework. *Front Neuroinform.* 2014;8:1–13.
31. Gupta V, Bustamante M, Fredriksson A, et al. Improving left ventricular segmentation in four-dimensional flow MRI using intramodality image registration for cardiac blood flow analysis. *Magn Reson Med.* 2018;79(1):554–560.
32. Bird RB, Stewart WE, Lightfoot EN. *Transport Phenomena*. 2nd editio. New York: John Wiley & Sons, Inc.; 2002.
33. Fenster BE, Browning J, Schroeder JD, et al. Vorticity is a marker of right ventricular diastolic dysfunction. *Am J Physiol - Hear Circ Physiol.* 2015;309(6):H1087–H1093.
34. Kamphuis VP, van der Palen RLF, de Koning PJH, et al. In-scan and scan–rescan assessment of LV in- and outflow volumes by 4D flow MRI versus 2D planimetry. *J Magn Reson Imaging.* 2018;47(2):511–522.
35. Mulchrone A, Bellofiore A, Douwes JM, et al. Impaired right ventricular-vascular coupling in young adults born preterm. *Am J Respir Crit Care Med.* 2020;201(5):615–618.
36. Mohlkert LA, Hallberg J, Broberg O, et al. The preterm heart in childhood: Left ventricular structure, geometry, and function assessed by echocardiography in 6-year-old survivors of perivable births. *J Am Heart Assoc.* 2018;7(2).
37. Joshi S, Wilson DG, Kotecha SSSS, Pickerd N, Fraser AG, Kotecha SSSS. Cardiovascular function in children who had chronic lung disease of prematurity. *Arch Dis Child Fetal Neonatal Ed.* 2014;99(5):373–379.
38. Suursalmi P, Eerola A, Poutanen T, Korhonen P, Kopeli T, Tammela O. Very low birthweight bronchopulmonary dysplasia survivors had similar cardiac outcomes to controls at six years to 14 years of age. *Acta Paediatr Int J Paediatr.* 2017;106(2):261–267.
39. Morsing E, Liuba P, Fellman V, Maršál K, Brodzki J. Cardiovascular function in children born very preterm after intrauterine growth restriction with severely abnormal umbilical artery blood flow. *Eur J Prev Cardiol.* 2014;21(10):1257–1266.
40. Kowalski RR, Beare R, Doyle LW, et al. Elevated blood pressure with reduced left ventricular and aortic dimensions in adolescents born extremely preterm. *J Pediatr.* 2016;172:75-80.e2.
41. Zivanovic S, Pushparajah K, Calvert S, et al. Pulmonary Artery Pressures in School-Age Children Born Prematurely. *J Pediatr.* Elsevier Inc.; 2017;191:42-49.e3.
42. Bensley JG, Stacy VK, De Matteo R, Harding R, Black MJ. Cardiac remodelling as a result of pre-term birth: Implications for future cardiovascular disease. *Eur Heart J.*

2010;31(16):2058–2066.

43. Bertagnolli M, Huyard F, Cloutier A, et al. Transient neonatal high oxygen exposure leads to early adult cardiac dysfunction, remodeling, and activation of the Renin-Angiotensin system. *Hypertension*. 2014;63(1):143–150.
44. Le B, Ferreira P, Merchant S, et al. Microarchitecture of the hearts in term and former-preterm lambs using diffusion tensor imaging . *Anat Rec*. 2020;(March):1–15.
45. Leeson P, Lewandowski AJ. A New Risk Factor for Early Heart Failure: Preterm Birth. *J Am Coll Cardiol*. 2017;69(21):2643–2645.
46. Sjöberg P, Bidhult S, Bock J, et al. Disturbed left and right ventricular kinetic energy in patients with repaired tetralogy of Fallot: pathophysiological insights using 4D-flow MRI. *Eur Radiol. European Radiology*; 2018;28(10):4066–4076.
47. Barker N, Fidock B, Johns CS, et al. A Systematic Review of Right Ventricular Diastolic Assessment by 4D Flow CMR. *Biomed Res Int*. 2019;2019.

## Tables

**Table 1. Baseline Anthropometric Measures**

	<b>Term (n=21)</b>	<b>Preterm (n=35)</b>	P-value
Male (n, %)	10, 48%	12, 34%	0.32
Chronological age (years)	25.1 (2.6)	25.9 (3.7)	0.23
Gestational age (weeks)	39.9 (1.0)	28.9 (2.7)	<b>&lt;0.001</b>
Height (m)	1.73 (0.08)	1.67 (0.09)	<b>0.05</b>
Weight (kg)	68.9 (9.0)	68.3 (14.9)	0.46
BSA ( $m^2$ )	1.8 (0.2)	1.8 (0.2)	0.24
BMI ( $kg/m^2$ )	23.0 (1.7)	24.3 (4.2)	0.24
Systolic BP (mmHg)	115.1 (8.7)	114.4 (10.8)	0.77
Diastolic BP (mmHg)	69.3 (6.8)	71.6 (7.2)	0.32

**Table 1:** Data are expressed as mean (SD). P-values by unpaired Wilcoxon Rank Sum tests.

Abbreviations: BSA, body surface area; BMI, body mass index; BP, blood pressure.

**Table 2. Cardiac MRI Structure and Function from BSSFP Cine Images**

	<b>Term (n=21)</b>	<b>Preterm (n=35)</b>	<b>P-value</b>
<b>Global Measures</b>			
HR (bpm)	65.6 (11.0)	71.8 (11.8)	0.06
SVi (mL/m <sup>2</sup> )	54 (10)	47 (7)	<b>&lt;0.01</b>
CI (L/min/m <sup>2</sup> )	3.54 (0.87)	3.35 (0.72)	0.66
<b>Ventricular Structure &amp; Function</b>			
LV EDVi (mL/m <sup>2</sup> )	81 (14)	73 (10)	0.06
LV ESVi (mL/m <sup>2</sup> )	27 (9)	26 (6)	0.97
LV EF (%)	67 (7)	64 (5)	0.11
LV E-Wave PFR/EDV (1/s)	3.5 (0.7)	3.5 (0.7)	1.00
LV A-Wave PFR/EDV (1/s)	1.0 (0.4)	0.9 (0.4)	0.68
LV E/A Filling Ratio	5.0 (4.6)	4.3 (1.8)	0.77
RV EDVi (mL/m <sup>2</sup> )	90 (18)	80 (14)	0.07
RV ESVi (mL/m <sup>2</sup> )	36 (12)	33 (9)	0.46
RV EF (%)	60 (8)	59 (6)	0.57
RV E-Wave PFR/EDV (1/s)	2.8 (0.6)	2.6 (0.6)	0.31
RV A-Wave PFR/EDV (1/s)	1.1 (0.5)	1.3 (0.6)	<b>0.04</b>
RV E/A Filling Ratio	3.5 (2.5)	2.3 (1.3)	<b>0.03</b>
<b>Atria Structure &amp; Function</b>			
LA ESVi (mL/m <sup>2</sup> )	32.5 (9.1)	26.7 (10.8)	<b>&lt;0.01</b>
LA EDVi (mL/m <sup>2</sup> )	13.2 (4.3)	11.2 (4.9)	0.07
LA SVi (mL/m <sup>2</sup> )	19.3 (6.1)	15.5 (7.6)	<b>0.01</b>
LA EF (%)	59 (7)	57 (12)	1.00
RA ESAi (mL/m <sup>2</sup> )	10.4 (2.0)	9.5 (1.9)	0.15
RA EDAi (mL/m <sup>2</sup> )	5.5 (1.5)	5.2 (1.2)	0.47
RA FAC (%)	46 (14)	45 (10)	0.35

**Table 2:** Data are expressed as mean (SD). P-values by unpaired Wilcoxon Rank Sum tests. All volumes and areas were indexed to body surface area. Abbreviations: HR, heart rate; CO, cardiac output; CI, cardiac index; EDV, end diastolic volume; ESV, end systolic volume; SV, stroke volume; EF, ejection fraction; PFR, peak filling rate (derived from volume-time curves); ESA, end systolic area on 4-chamber view; EDA: end diastolic area on 4-chamber view; FAC, fractional area change.

**Table 3. 4D Flow MRI Measures of Ventricular Hemodynamics**

	<b>Term (n=21)</b>	<b>Preterm (n=35)</b>	<b>P-value</b>
<b>Ventricular Kinetic Energy</b>			
LV Average KE/EDV ( $\mu\text{J}/\text{mL}$ )	11.7 (2.7)	13.3 (4.4)	0.13
LV Peak Systolic KE/EDV ( $\mu\text{J}/\text{mL}$ )	21.1 (6.9)	22.2 (6.6)	0.42
LV E-Wave KE/EDV ( $\mu\text{J}/\text{mL}$ )	41.9 (11.1)	42.3 (15.8)	0.91
LV A-Wave KE/EDV ( $\mu\text{J}/\text{mL}$ )	9.1 (6.7)	12.7 (9.9)	0.14
LV E/A KE Ratio	6.5 (4.2)	4.8 (3.3)	0.06
RV Average KE/EDV ( $\mu\text{J}/\text{mL}$ )	8.8 (2.3)	9.8 (3.5)	0.16
RV Peak Systolic KE/EDV ( $\mu\text{J}/\text{mL}$ )	29.5 (9.6)	31.9 (14.3)	0.73
RV E-Wave KE/EDV ( $\mu\text{J}/\text{mL}$ )	15.2 (5.7)	13.4 (4.7)	0.41
RV A-Wave KE/EDV ( $\mu\text{J}/\text{mL}$ )	4.9 (2.1)	7.5 (5.8)	<b>0.05</b>
RV E/A KE Ratio	3.5 (1.4)	2.4 (1.7)	<b>&lt;0.01</b>
<b>Atrioventricular Valve Inflow</b>			
MV Net flow/BSA (L/min/m <sup>2</sup> )	2.8 (0.5)	2.7 (0.7)	0.73
MV E-Wave Flow/BSA (L/min/m <sup>2</sup> )	12.4 (3.5)	11.9 (3.5)	0.54
MV A-Wave Flow/BSA (L/min/m <sup>2</sup> )	3.1 (1.2)	3.3 (1.1)	0.44
MV E/A Flow Ratio	4.9 (3.6)	4.2 (3.1)	0.48
TV Net flow/BSA (L/min/m <sup>2</sup> )	2.8 (0.8)	2.7 (0.7)	0.75
TV E-Wave Flow/BSA (L/min/m <sup>2</sup> )	6.7 (2.0)	6.3 (1.8)	0.85
TV A-Wave Flow/BSA (L/min/m <sup>2</sup> )	3.0 (1.0)	3.6 (1.3)	0.11
TV E/A Flow Ratio	2.4 (1.0)	2.0 (1.1)	0.07
<b>Viscous Energy Dissipation Rate <math>E'_L</math></b>			
LV Net $E'_L$ /EDV ( $\mu\text{J}/\text{mL}$ )	4.5 (2.9)	6.1 (4.9)	0.26
LV Peak Systolic $E'_L$ /EDV ( $\mu\text{W}/\text{mL}$ )	7.3 (6.0)	11.1 (9.4)	0.06
LV E-Wave $E'_L$ /EDV ( $\mu\text{W}/\text{mL}$ )	14.0 (7.9)	18.9 (17.9)	0.29
LV A-Wave $E'_L$ /EDV ( $\mu\text{W}/\text{mL}$ )	6.9 (8.4)	11.5 (13.3)	0.22
LV E/A Ratio	3.6 (2.2)	3.0 (2.2)	0.15
RV Net $E'_L$ /EDV ( $\mu\text{J}/\text{mL}$ )	1.9 (0.6)	2.4 (1.0)	<b>0.02</b>
RV Peak Systolic $E'_L$ /EDV ( $\mu\text{W}/\text{mL}$ )	4.2 (1.6)	5.7 (3.0)	<b>0.03</b>
RV E-Wave $E'_L$ /EDV ( $\mu\text{W}/\text{mL}$ )	3.8 (1.5)	4.5 (2.5)	0.53
RV A-Wave $E'_L$ /EDV ( $\mu\text{W}/\text{mL}$ )	2.2 (1.6)	3.9 (4.0)	<b>0.03</b>
RV E/A $E'_L$ Ratio	2.2 (0.9)	1.7 (1.2)	0.06

**Table 3:** Data are expressed as mean (SD). P-values by unpaired Wilcoxon Rank Sum tests.

Abbreviations: KE, kinetic energy; EDV, end diastolic volume; LV, left ventricle; RV, right ventricle;

MV, mitral valve; TV, tricuspid valve; BSA, body surface area;  $E'_L$ , viscous energy dissipation rate;  
 $E_L$ , net viscous energy dissipation.

## Figures

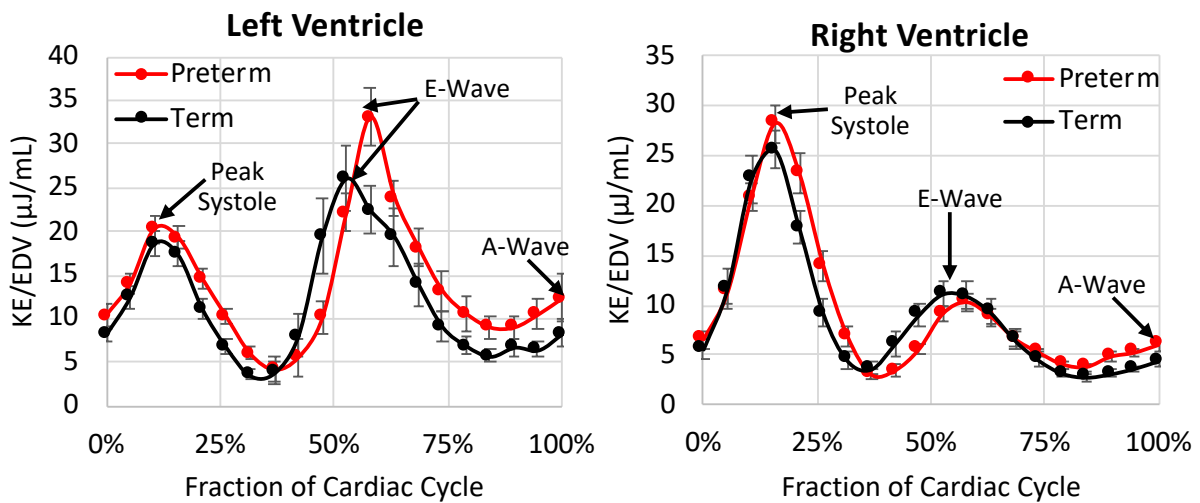


**Figure 1:** Normalized kinetic energy vs. time graphs for each birth status. Dots represent mean within each subject group and error bars represent standard deviation. The KE-time curves show three peaks: 1 systolic peak, 1 early diastolic peak (E-wave), and 1 late diastolic peak coinciding with atrial contraction (A-wave). The KE/EDV value at each of these peaks was recorded for each subject, along with the average KE/EDV value over the cardiac cycle. Abbreviations: KE – kinetic energy; EDV – end diastolic volume.

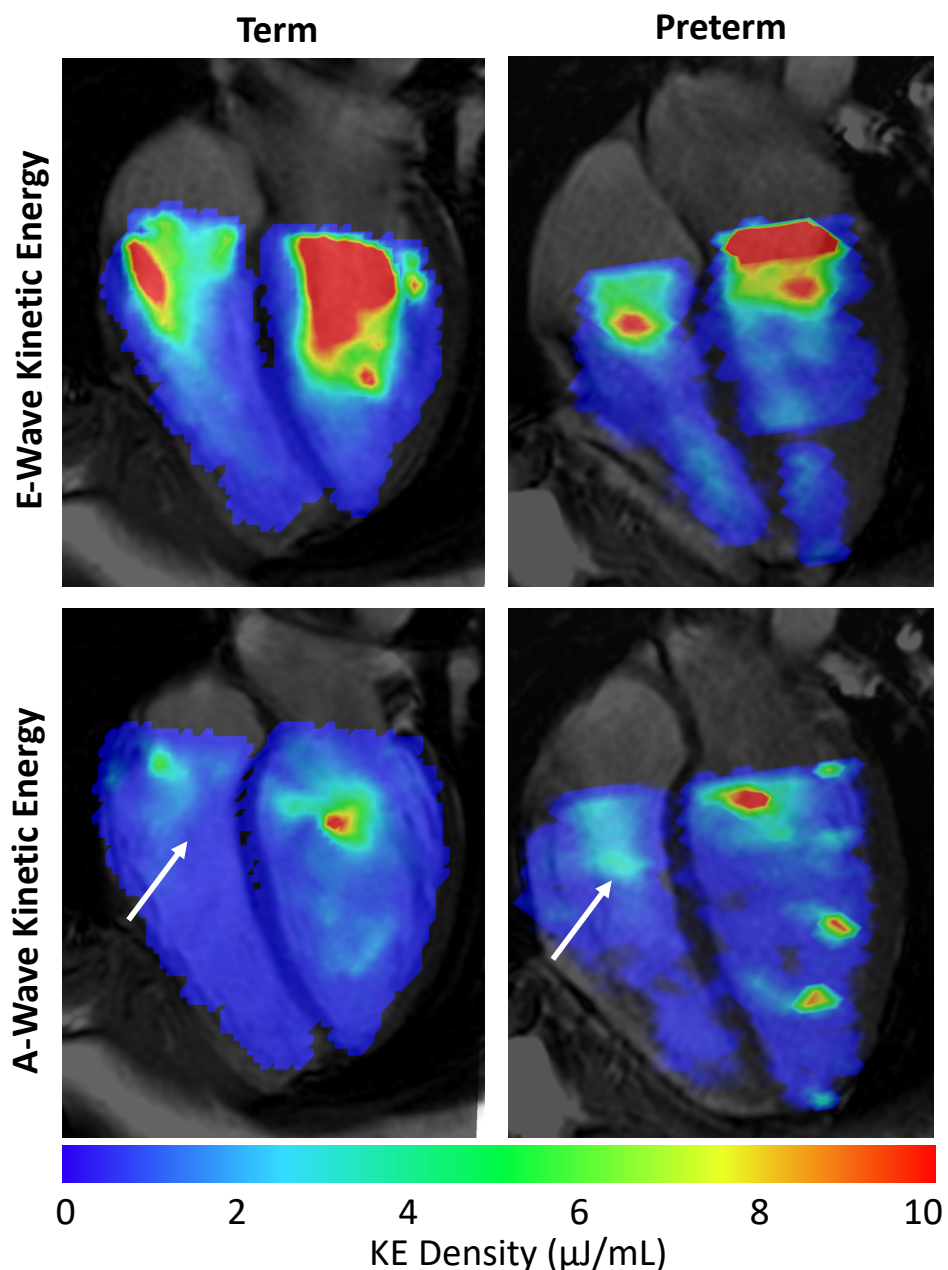


**Figure 2:** Kinetic energy (KE) maps for single slices through 2 representative subjects: 1 term-born (left column) and 1 preterm-born (right column). The top row is a snapshot at the E-wave (early diastolic KE peak) and the bottom row is a snapshot at the A-wave (late diastolic KE peak). The preterm-born subject exhibited more KE in the RV at the A-wave phase (white arrows). Abbreviations: KE – kinetic energy; RV – right ventricle.

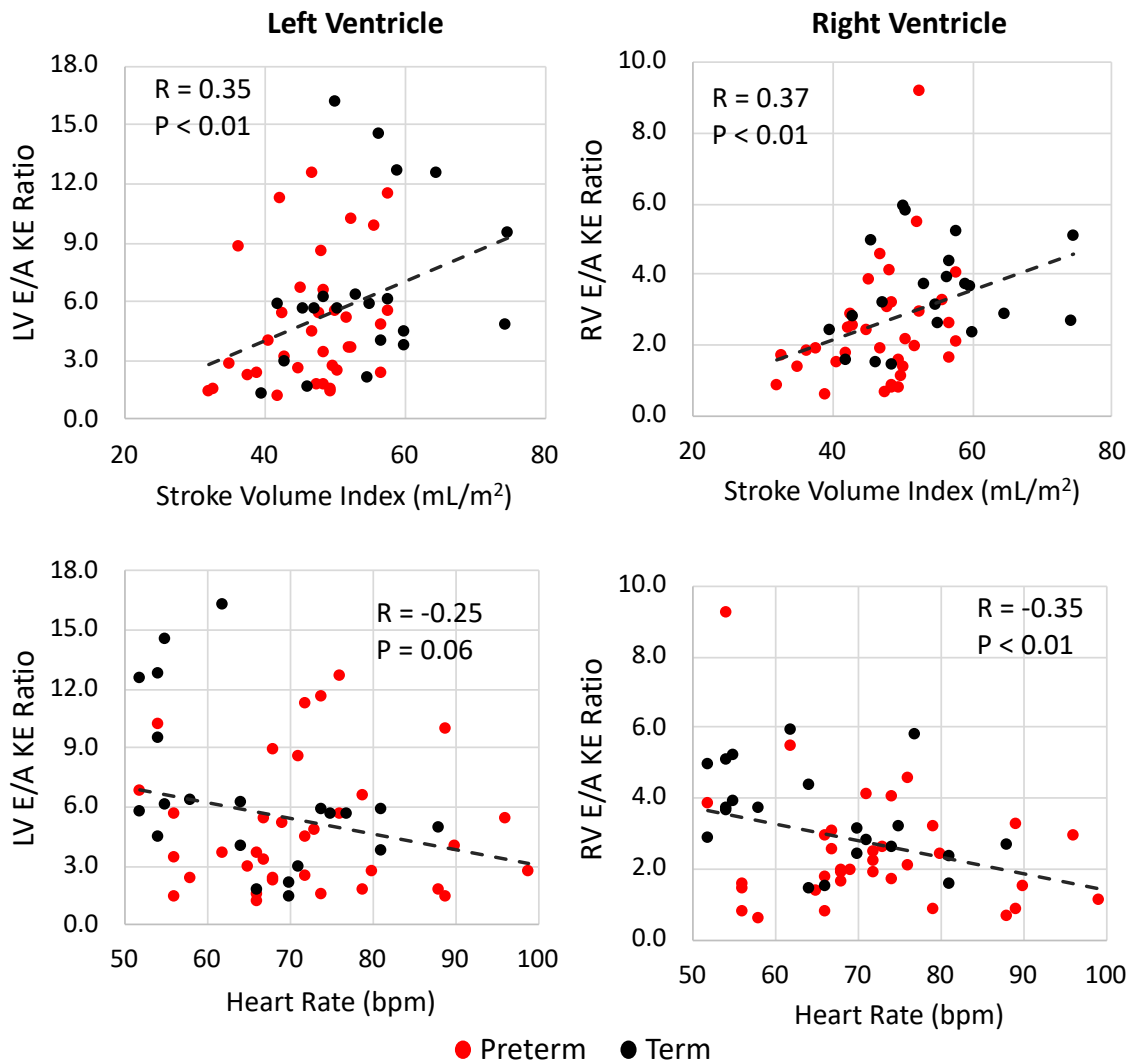


**Figure 3:** Scatter plots of LV (left column) and RV (right column) E- to A-wave KE ratio vs. stroke volume index (top row) and heart rate (bottom row). Abbreviations: LV – left ventricle; RV – right ventricle; KE – kinetic energy; PAP – pulmonary artery pressure; E/A Ratio – ratio of early diastolic peak to late diastolic peak; EDVi — end diastolic volume index.